ACOUSTIC INTERACTIONS WITH INTERNAL STRESSES IN METALS

O. Buck and R. B. Thompson
Science Center, Rockwell International
Thousand Oaks, California 91360

It became evident at the residual stress meeting in San Antonio last year[1] that it is necessary to restate the definitions for internal stresses.[2] In general, we are talking about three kinds of residual stresses as shown in Table I. The one that's called the first kind of internal stress ranges over millimeters or centimeters (or long range internal stress) and can be identified by x-rays through a line shift. The second kind ranges over dimensions of microns and with the x-ray method gives rise to a shift as well as a line broadening. This type is usually due to particles within the material or particles of a different phase or something similar. The third kind, which ranges over 100 to 1,000 Angstroms, is a microscopic internal stress in a true sense and is indicated by x-ray line broadening only. In the following, we will be talking about the internal stresses of the third kind, due to dislocations, and later about the first kind of internal stresses.

Kind	Range	X-Ray	Examples
1st	Macroscopic (Order μm to cm)	Line shift	Elastic deformation of a cut and rewelded toroid. Thermal stresses.
2nd	(Order μm) Microscopic	Line shift and line broadening.	Particles of different phases in a matrix.
3rd	(Order 100-1000Å)	Line broadening.	Edge and screw dislocations (plastic deformation).

Table I. Classification of internal stresses.

Why do we talk about the third kind of internal stresses in connection with dislocations? I will use the elastic model of a dislocation, and for simplicity, let's just use the model of a screw dislocation, which is the simplest case that you can have. This model is a cylinder cut along the axis as shown in Fig. 1. A displacement of one of the surfaces against the other parallel to the axis (a Burgers vector) and a rewelding of these surfaces, yields a stress field that will drop off as 1/R over a range of 100 to 1,000 Å. The third kind of internal stresses is of practical importance since these are the stresses which determine the flow stress of a material during deformation and during fatigue. They also determine fatigue softening or hardening effects depending on how the dislocation structure is altered. As was pointed out before in this meeting, one would like to have a nondestructive method for determining these kinds of internal stresses since it would allow the measurement of such parameters as yield stress and perhaps even fracture toughness without destroying the material.
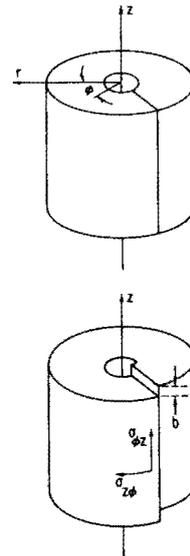

Figure 1. Model of a "screw" dislocation. The cylinder in the top part of the figure is cut along a radial direction. An offset b, as shown in the bottom part of the figure, and rewelding generates an internal stress field, given by Equation (1).

Let us define the internal stresses due to dislocations and their meaning in more detail. The model, defined in Fig. 1, yields a stress field given by

$$\sigma_G = \frac{bG}{2\pi R} \qquad (1)$$

with b = Burgers vector and G the shear modulus. R will be of the order of the loop length L of the dislocations. As has been established before,[3] one of the methods that can be used to determine the internal stresses due to dislocations is that of acoustic harmonic generation. As will be discussed later, the harmonic amplitude is a function of L and thus, the internal stress. Basically, an ultrasonic wave launched at one side of a crystal will become distorted as it travels through the crystal due to nonlinearities within the crystal. There are two nonlinear contributions to this distortion. The first one is due to the anharmonicity of the lattice. This is a very well known contribution since it is the same one which gives rise to the thermal expansion coefficient. Almost all lattices contain dislocations which bow out under stress and give rise to a nonlinearity. Both types of nonlinearities contribute to second harmonic generation[4] as shown in the next equation.

$$U_2 = U_1^2 \, \omega^2 a \, (\text{Lattice} + KL^2) \qquad (2)$$

The second harmonic amplitude U_2 increases with the square of the fundamental amplitude U_1 as well as ω^2 (ω being 2π times the frequency of the acoustic wave). As you can see, the higher the frequency the better the sensitivity of the measurement (our equipment operates close to 30 MHz). Furthermore, the term a is the propagation distance of the wave. The terms in the brackets are the lattice part, determined by second and third order elastic constants and the dislocation part KL^2 with L being the dislocation loop length, and K a proportionality constant.

Using Eqn. 1, and replacing R by L, we can calculate the second harmonic amplitude due to dislocations, U_{2d}. In other words, $U_{2d} = U_2 - U_2 \text{lattice}$ is the second harmonic in terms of the internal stresses of the third kind. We find that U_{2d} is proportional to σ_G^{-2}, going back to Eqn. 1 again, or also that U_{2d} is proportional to $(\sigma - \sigma_0)^{-2}$, since[3] $\sigma_G \approx \sigma - \sigma_0$ (σ = flow stress, σ_0 = yield stress.)

Each crystal contains a certain dislocation arrangement typical of the crystal's state of deformation. In the above terms, there is a certain stress distribution (third kind of internal stresses) which is symbolized in Fig. 2. The arrangement may contain dislocation pile-ups of both negative as well as positive dislocations (determined by the sign of the Burgers vector), which gives rise to an oscillating internal stress. As you see, this stress field averages out to zero. The wavelength of these oscillations is in the neighborhood of 100 to 1,000 Å.

In the following, I will discuss measurements of these internal stresses by second harmonic generation. I talked about the technique last year[5] so let us just concentrate on the results. Using a virgin aluminum single crystal we expect the second harmonic amplitude to be high since the loop length L in Eqn. 2 is large (dislocation density about 10^6 cm^{-2}). As we apply a compressive stress σ which exceeds the yield stress σ_0 of the material, one expects a change in the observed second harmonic amplitude. Since the dislocation density goes up during plastic deformation, the loop length goes down. From the above discussion, we expect that with increasing deformation the dislocations will see an increasing internal stress field, indicated by a decreasing second harmonic amplitude. As shown in Fig. 3, harmonic generation indeed decreases with increasing applied stress for stresses above σ_0. Below σ_0 the situation is reversed since in the elastic range the dislocation loop length becomes larger due to dislocation bowing out under the applied stress[4]. Harmonic generation is defined in Fig. 3 as the ratio of the total received second harmonic amplitude U_2 over the fundamental amplitude U_1. U_2 is the sum of the harmonic amplitude due to a lattice contribution (U_{2e}) and the amplitude produced by dislocations (U_{2d}), as given by Eqn (2). The lattice contribution to U_2/U_1 should be independent of applied stress and has been drawn as the horizontal dashed line in Fig 3. Qualitative verification of the dislocation contribution U_{2d} to harmonic generation above σ_0 in agreement with Eqn (2) is the major point made here.

Figure 3. Normalized second harmonic displacement versus compressive stress (in multiples of the yield stress σ_0) for 30 MHz longitudinal waves along the [100] direction of aluminum. A second coordinate system has been introduced to show these data.
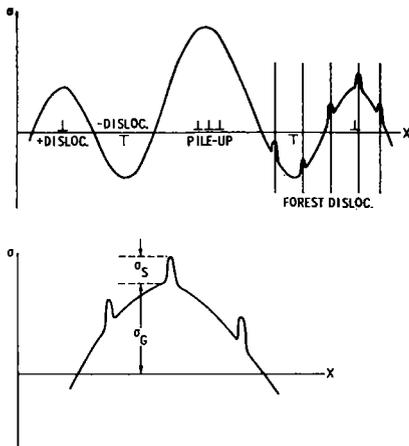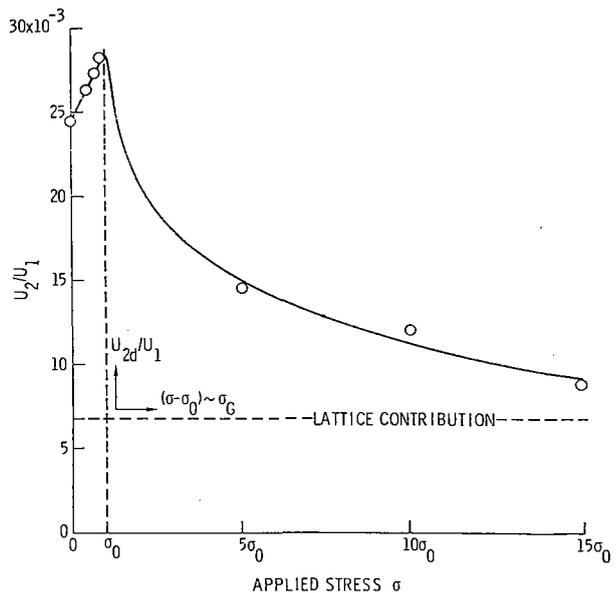
Figure 2. A dislocation arrangement, consisting of + and - dislocations as well as a dislocation pile-up generates a sinusoidally varying stress field, the amplitude of which depends on the number of dislocations in the group. "Forest" dislocations give rise to additional stress-spikes (top of the figure). A dislocation pressed against this stress field has to overcome a total stress $\sigma = \sigma_G + \sigma_S$ (bottom of the figure).

After the compression tests, shown in Fig. 3, the crystal was fatigued at a maximum stress level of 7.5 σ_0 and the harmonic generation was determined as a function of fatigue cycles applied to the aluminum. Since it was impossible to determine the flow stress of the material after different degrees of fatigue directly, the surface hardness was measured using a Knoop hardness indenter. Basically, the harmonic generation increased and Knoop hardness decreased as fatigue proceeded. These results are shown in Fig. 4 in the form U_2/U_1 versus Knoop hardness to demonstrate the qualitative features expected from Eqn. (2). In terms of the dislocation parameters, the result can be interpreted in the following way. The dislocation loop length in the present case is quite short prior to fatigue. Long loops develop during fatigue and yield an increased contribution to the second harmonic; thus harmonic generation reflects the internal stresses (at least within the "dislocation cells") as fatigue proceeds.
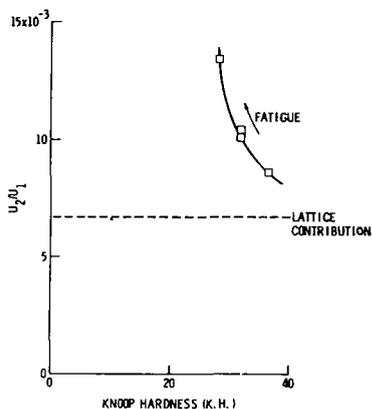

Figure 5. The effect of fatigue on second harmonic generation in Al 2219 T851 at various maximum load levels.

Figure 4. Normalized second harmonic displacement versus Knoop hardness during fatigue of a deformed Al single crystal (σ_{max} = 7.5σ_0, σ_{min} =0.8 σ_0).

Effects of fatigue on harmonic generation in the high strength alloy Al 2219-T851 were studied over a relatively wide range of maximum stress levels (0.8$\sigma_y \leq \sigma_{max} \leq$ 1.1σ_y with σ_y being the yield stress). The results, shown in Fig. 5, indicate that within the accuracy of the measurements fatigue of a high strength aluminum produces no systematic change in the second harmonic amplitude. To be sure that the absence of an effect was not caused by (the somewhat unusual) compression-compression type fatigue, similar experiments were performed on Al 6061-T6 fatigued in tension-compression at 20 KHz with an ultrasonic horn arrangement. Again, within the accuracy of our measurements, no change in the second harmonic was observed.
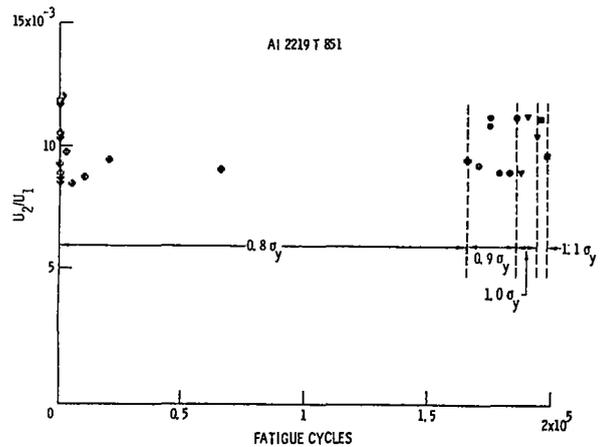
These results demonstrate the limitations of our present method: it is speculated that in this type of material the diffusion of interstitals at room temperature causes repinning of dislocations in aluminum, thus effectively preventing changes in acoustic harmonic generation. In materials like Ti-alloys and steels, such immediate repinning may not be expected. As can be clearly seen from the results[6] on Ti-alloys and steel replotted in Fig. 6, the generation of a second harmonic seems to be a useful quantity to determine the remaining life of the specimen. Experiments using these materials are presently underway and are aimed at understanding the responsible mechanisms of second harmonic generation of Ti-alloys and steels.
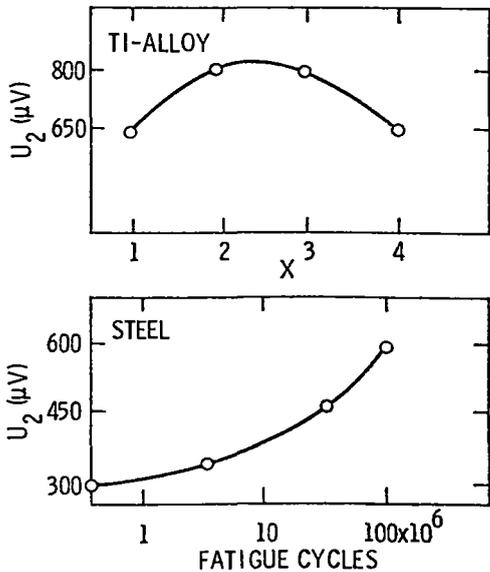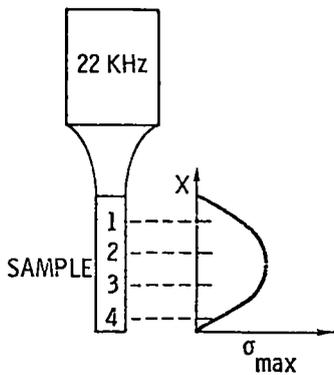
Figure 6. Top: Experimental 20 KHz arrangement to generate fatigue.

Middle: Amplitude of second harmonic (U_2) as a function of extent of fatigue (positions 1 and 4 - low stress amplitudes, positions 2 and 3 - high stress amplitudes).

Bottom: U_2 as a function of fatigue at maximum stress amplitude [after Ref. (6)].

The present results on second harmonic generation in Al and Al alloys can be summarized as follows:

(1) Theory and experiments demonstrate that acoustic harmonic generation in bulk waves could be a useful tool to nondestructively test the flow stress and the state of fatigue as long as processes are involved in which the free dislocation loop is changed. Using an Al single crystal as a model system, theoretical semiquantitative correlations have been verified. Limitations on the applicability of the method in the case of Al alloys have been studied. Alloy additions apparently repin the dislocations immediately, due to a low activation energy of motion, and no effect can be observed.

(2) In materials where acoustic harmonic generation is sensitive to fatigue, the major part of the change occurs in the very early part of the fatigue life concomitant with a fatigue hardening or softening effect. In the latter part of the fatigue life where microcrack initiation and propagation takes place (saturation stage of fatigue), changes of the bulk properties are minor so that harmonic generation is affected very little.

I'd like to describe a second way in which we are using ultrasonic waves to detect residual stresses. I'll primarily be concerned with the longer range stresses associated with bending, shot peening, drawing, or other macroscopic effects, rather than the short range microscopic stresses just discussed. My comments will be directed specifically at ferromagnetic materials. For these materials, there are a number of magnetic parameters which have already been studied as possible indicators of stress.[1] However, one set of parameters that are rather sensitive to stress, but which have not been utilized before, are the magnetostrictive properties of a ferromagnetic material. Figure 7 shows static magnetostriction data for Armco iron.[7] For zero stress, a sample first lengthens and then shortens during magnetization. However, for a relatively modest tension of 10 ksi, the initial lengthening is suppressed, and the material only shortens during magnetization. On the other hand, for a compressive stress of the same magnitude, lengthening is enhanced.
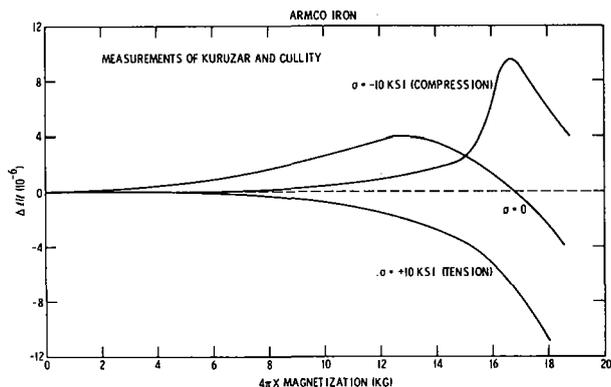

Figure 7. Changes in the magnetostriction of iron induced by tensile and compressive stress.

The differences between the three cases are striking. We have found that electromagnetic transducers for generating ultrasonic waves can be used to nondestructively measure this stress-sensitive magnetostrictive response. The detailed experimental configuration is illustrated in Fig. 8. An electromagnetic transducer consists of a meander coil carrying a dynamic current, which establishes dynamic magnetic fields in the sample, and

an electromagnet which produces a variable bias magnetic field. Such a transducer, through the magnetostrictive effect, launches an ultrasonic surface wave which is detected by any means convenient, for example, a piezoelectric wedge transducer. The amplitude of the detected wave is proportional to the differential magnetostrictive coefficients of the material and thereby is related to the stress through the physical effect that was illustrated in Fig. 7.
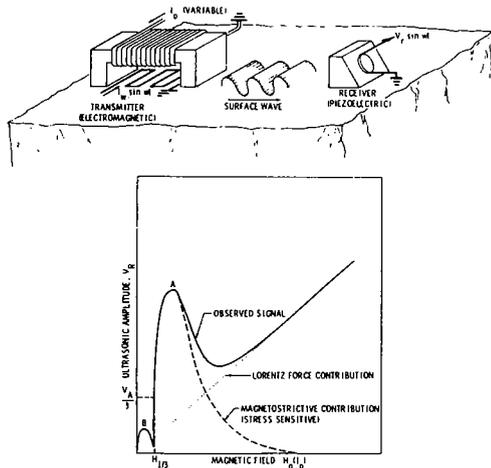

Figure 8. Experimental apparatus for determining efficiency of electromagnetic generation of surface waves as a function of magnetic field. The major features observed in ferrous materials are shown in the schematic efficiency plot below.

The bottom of Fig. 8 illustrates a typical magnetic field dependence of transducer efficiency. At high fields, there is a linear relation between the applied field and the received signal strength. This is caused by the Lorentz force generation process, which is dominant when the material is magnetically saturated. It occurs in all metals and is not of use in the detection of stress.

At lower fields there is considerable structure in the efficiency plot. The two peaks shown are typical for iron. Their origin can be explained by referring to models for transducer efficiency[8] which demonstrate that the amplitude of the generated wave is proportional to the differential magnetostriction of the material. From Fig. 7 it will be noted that there are two regions of large differential magnetostriction, one when the material is rapidly lengthening, and another while the material is shortening. These produce the two peaks in efficiency. The stress-induced changes in these features in Fig. 7 produce changes in transduction efficiency, which can be measured by an apparatus such as the one shown in Fig. 8.

Figure 9 summarizes the physics of the stress sensitivity. Recall that the orientation of the magnetic moments in a ferromagnetic body are determined, among other things, by the magnetic anisotropy energy. A three-dimensional plot of this energy for iron is shown at the top of the figure.[9] The energy is minimum when the magnetization is aligned along the cube axis, the so-called easy axes of magnetization. The energy is maximum when the magnetization is aligned along the body diagonals. The lower figure shows the anisotropy energy for particular planar cuts of this surface. The solid line shows the energy when there is no applied stress. The dotted line shows the energy when a tensile stress of 30 ksi is applied along the [100] axis. It can be seen that the magnetic energy is changed appreciably.
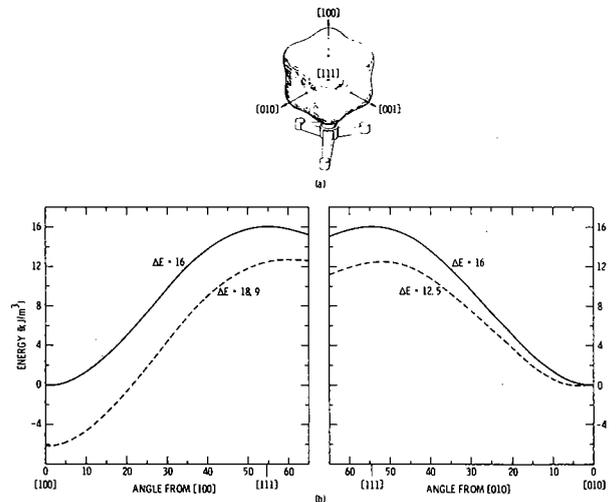

Figure 9. Anisotropy energy of iron; (a) three dimensional plot of energy versus angle, (b) planar cuts of energy surface with zero stress (solid line) and a tensile stress of 200MN/m² (29 KSI) along the [100] axis (broken line).

Two aspects should be emphasized. With no stress the energy minima along the [100] and [010] axes are of equal depth. This is not the case in the presence of stress, and there will be a preferential tendency for the magnetic moment to orient along the [100] axis, rather than the [010] or [001] axes. This influences the detailed distribution of domains and hence influences the magnetostrictive as well as other magnetic responses at low fields.

There is also a change in the effective magnetic anisotropy, i.e., the difference between the maximum and minimum energy points. This will influence the magnetic response at high fields, since changes are produced by field induced rotations of the magnetization against this anisotropy.

We have measured the stress dependence of the transducer efficiency in a number of materials. We have looked at three iron-nickel alloys: iron, nickel, invar. A detailed discussion is beyond the scope of this talk. However, it should be noted that the stress effects in invar and nickel are actually much larger than those in iron and carbon steel, which I am going to deal with today. Figure 10 shows the stress dependence of the transduction efficiency in Armco iron. For no stress, there is a large efficiency and a small peak B, as indicated by the solid line. When a tensile stress is applied, peak B is depressed and the rapid change in efficiency between peaks A and B moves to lower fields, as indicated by the dashed line. Conversely, the presence of a compressive stress enhances peak B, moves the rapid change in efficiency to higher fields, and changes some of the features at high fields.
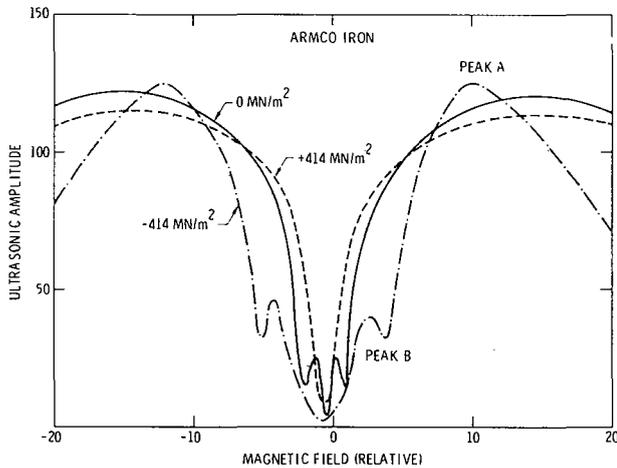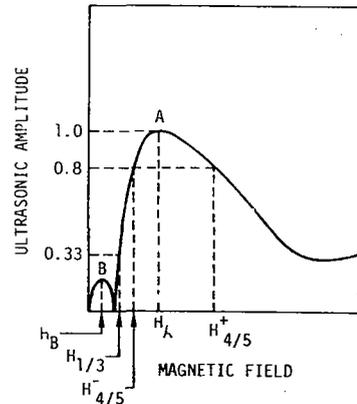

Figure 11. Definition of stress sensitive parameters.

These are rather ad hoc definitions, but they have yielded some very useful results. The variations of each of the parameters shown in Fig 11 as a function of stress have been measured in several materials. The two most useful have been $H_{4/5}^{\pm}$ and $H_{1/3}$.

Figure 12 shows the value of $H_{1/3}$ as a function of stress for two materials: Armco iron and 1018 steel.[10] The stress was applied by bending the sample, so the tension data were taken on a different side of the sample than the compression data. The offset in the data was caused by the presence of different residual stresses produced in the two sides of the sample by the forming process.

Figure 10. Efficiency plot in Armco iron for zero applied stress and calculated stresses of + 414 MN/m² (+60 KSI). The absolute magnetic field is approximately 300 Oesteds at peak A.

In order to quantitatively study the stress effects, we have defined some phenomenological parameters from the efficiency plot, as shown in Fig. 11. Here the efficiency data has been normalized so that the value at peak A is unity. The magnetic field necessary to produce an efficiency that is a certain fraction of this maximum value B is then taken as the stress sensitive parameter. For example, $H_{4/5}^{\pm}$ is defined as the magnetic field necessary to produce an efficiency that is 4/5 or 80% of the efficiency at peak A. By choosing normalized parameters in this way, the efficiency measurement is made independent of propagation losses that would lead to errors in an absolute measurement.
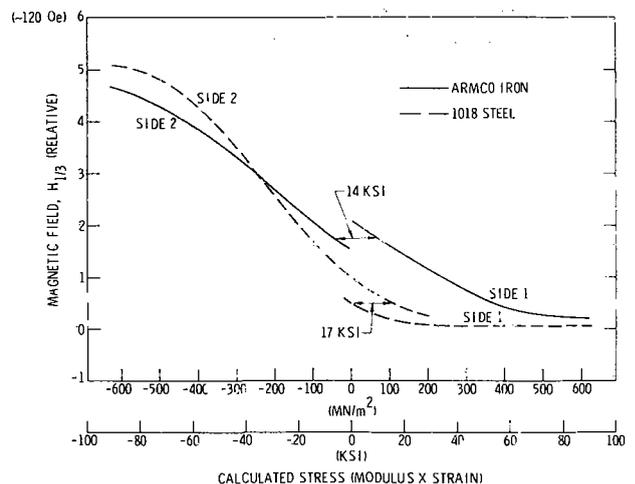

Figure 12. $H_{1/3}$ versus stress for Armco iron and 1018 steel.

The 1018 steel data here was reported at this meeting last year.[11] At that time, it was reported that the difference in stress implied by the offset in the data on the two sides was confirmed by independent x-ray measurements. Since that time, we have measured the Armco iron sample. The same basic phenomena were observed with slightly different details. In this case, however, x-ray measurements of stress were not consistent with the offset in the efficiency data. However, the x-ray data varied dramatically from point to point, and there was very heavy machining damage visible on the sample surface. It appears likely that there were rapid fluctuations of stress near the surface that were picked up by the x-rays, but not detected by the efficiency measurement which averages over a greater volume of material. (The efficiency technique senses the average stress under the transducer down to a depth equal to the electromagnetic skin depth.)

Inspection of Fig. 12 reveals that, although $H_{1/3}$ is quite sensitive to compressive stresses, it tends to be insensitive to tensile stresses. A second parameter, $H_{4/5}^{\pm}$, has just the opposite behavior. Figure 13 shows the variation of $H_{4/5}^{\pm}$ as a function of stress in two materials, A-366 steel, which is a cold rolled plate of low carbon steel, and A-569 steel, which is a hot rolled plate of the same nominal composition. In each case there is very little variation of $H_{4/5}$ for compressive stresses, but a very strong variation under tension. Two sets of experimental data are shown for each material. In one set, the stress and measurement axes were both parallel to the rolling direction, and in the second they were both perpendicular. The results for the two cases in A-569 steel were virtually identical, indicating that the effect is independent of texture in this material. This was not the case in the A-366 steel. However, one of the samples was inadvertently bent beyond the elastic limit during fabrication and hence had a built-in stress before the measurement was made. The differences between the responses of the two samples may be due to this history.
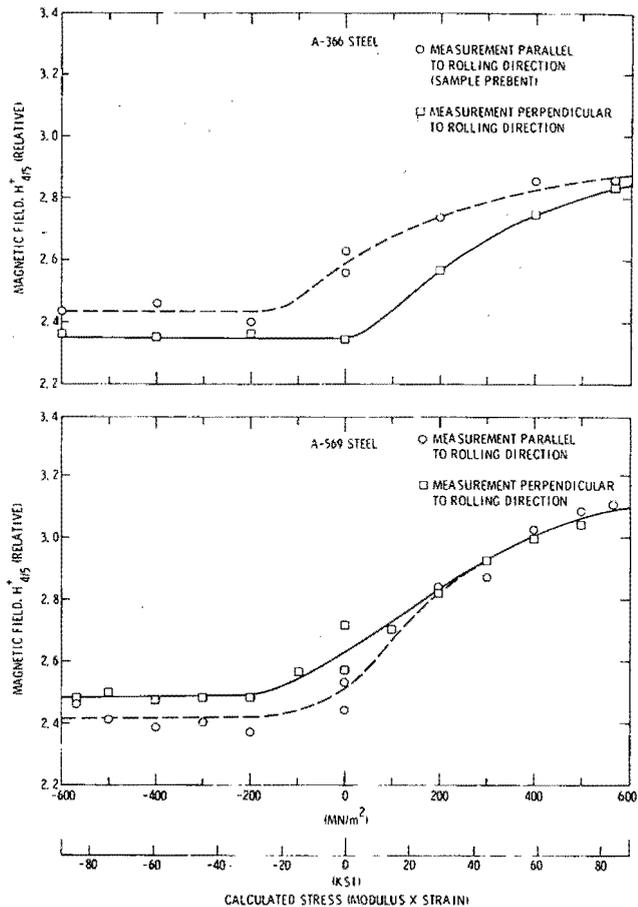

Figure 13. $H_{4/5}^{+}$ versus stress for A-366 and A-569 steel sheet cut both parallel and perpendicular to rolling direction.

Figure 14 shows the effect of rotating the direction of measurement with respect to the stress axis. For the A-569 steel, we see that both the $H_{1/3}$ and $H_{4/5}^{+}$ parameters exhibit large changes with stress when measurements are made parallel to the stress axis. However, the effect is very small when measurements are made perpendicular to the applied stress. This result should be useful in determining the axis as well as magnitude of an unknown stress.
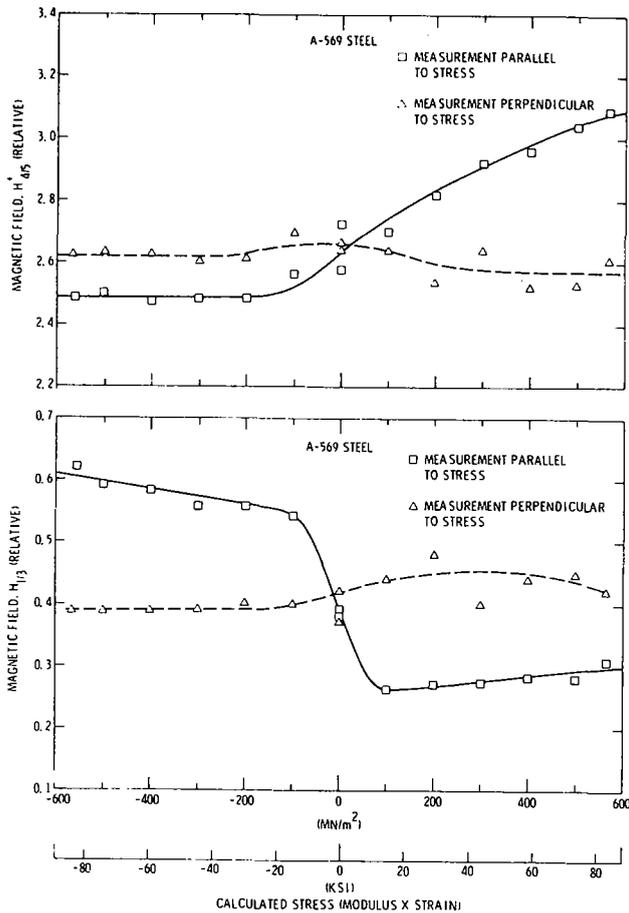
Figure 14. Effect of stress direction upon $H_{1/3}$ and $H_{4/5}{}^+$.

In summary, we have increased our understanding of the physics of the stress sensitivity of transducer efficiency; we have surveyed several materials; we have found a new parameter that we had not reported before, and we have looked at some orientation effects. Much more fundamental work is needed before we have a full understanding of this phenomena. However, the technique appears ready for development in specific applications where the material variations are well controlled.

REFERENCES

1. Proceedings of a Workshop on Nondestructive Evaluation of Residual Stress, San Antonio, Texas, August 1975, NTIAC-76-2.

2. A. Kochendorfer, Plastische Eigenschaften von Kristallen und metallischen Werkstoffen, Springer Verlag, Berlin, 1941.

3. O. Buck, IEEE Transactions on Sonics and Ultrasonics SU-23, 346 (1976)

4. A. Hikata, B. B. Chick, and C. Elbaum, Appl. Phys. Letters 3, 195 (1963)

5. R. B. Thompson, O. Buck, and D. O. Thompson, J. Acoust. Soc. Amer. 59, 1087 (1976)

6. J. V. Yermilin, L. K. Zarembo, V.A. Krasil'nikov, Ye. D. Mezintsev, V. M. Prokhorov, and K. V. Khilkov, Phys. Met. Metallogr. 36, No. 3, 1974(1973).

7. Michael E. Kuruzar and B.D. Cullity, Int. J. Magn. 1, 323 (1971).

8. R. Bruce Thompson, 1975 Ultrasonics Symposium Proceedings (IEEE, N.Y., 1975) p. 633.

9. R.M. Bozorth, Ferromagnetism (P. Van Nostrand, Inc., Princeton, 1951).

10. R. Bruce Thompson, Appl. Phys. Letters, 28. 483 (1975).

11. R. B. Thompson, Proceedings of the ARPA/ARML Review of Quantitative NDE, AFML-TR-75-212, p. 813.

We have also made a number of qualitative observations which can not be reported within this brief paper. For example, the $H_{4/5}{}^+$ parameter appears to be relatively insensitive to variations in microstructure, dislocation densities, and so forth of the material. This is presumably because the material is biassed to a point near saturation and consequently magnetic changes are essentially reversible and not strongly influenced by defects that tend to restrict Block wall motion at lower fields. Hence, this may be a very useful regime in which to measure an unknown material whose complete history and structure is not known. On the other hand, $H_{1/3}$ is quite sensitive to these effects. This appears to be somewhat of a disadvantage in the detection of stress, but may be quite useful in the detection of other important mechanical properties such as fatigue.

DISCUSSION

PROF. JOHN TIEN: Thank you, Bruce. Would you please address your questions to either Bruce or Otto.

MR. ROY SHARPE (Harwell Labs): Did I understand you to say that your method will distinguish between stress and preferred orientation, because this obviously is the major problem in other ultrasonic methods.

DR. BRUCE THOMPSON: The experiments which I reported demonstrated little effect of preferred orientation on the data. We have to do more work to quantify this, since these experiments were performed on a single alloy. We have not constructed the pole figure as yet to say in detail what the texture was, but I think we can assume there was some significant preferred orientation in that material. The results are quite encouraging.

PROF. TIEN: Otto, I have a question on your aluminum data. I guess you are saying what messed it up is the fact that diffusion was too fast?

DR. BUCK: Yes, that's what I believe has happened.

PROF. TIEN: So, you still see success if you went lower in temperature?

DR. BUCK: That is quite possible.

PROF. TIEN: So, consequently for any other material, if you go high in temperature, it might show up again.

DR. BUCK: That's right. The results should depend on the diffusion energy.

PROF. TIEN: That is interesting.